

# $^1\text{H}$ NMR and fluorescence studies of the complexation of DMPG by wheat non-specific lipid transfer protein. Global fold of the complex

Patrick Sodano<sup>a,\*</sup>, Anita Caille<sup>a</sup>, Denise Sy<sup>a,b</sup>, Grégoire de Person<sup>a</sup>, Didier Marion<sup>c</sup>, Marius Ptak<sup>a,b</sup>

<sup>a</sup>Centre de Biophysique Moléculaire, rue Charles Sadron, 45071 Orléans Cedex 02, France

<sup>b</sup>Université d'Orléans, rue de Chartres, P.O. Box 6759, 45067 Orléans Cedex 02, France

<sup>c</sup>Laboratoire de Biochimie et Technologie des Protéines, INRA, rue de la Géraudière, P.O. Box 1627, 44316 Nantes Cedex 05, France

Received 10 June 1997; revised version received 11 September 1997

**Abstract** Plant non-specific lipid transfer proteins (LTPs) are proteins which transfer lipids between membranes *in vitro* and are believed to be involved in the transport of cutin monomers to the cuticle layer *in vivo* or in the plant defence against phytopathogens. The complexation of DMPG, a diacyl phospholipid, by wheat ns-LTP, a protein extracted from wheat seeds, was followed by  $^1\text{H}$  NMR and fluorescence spectroscopy. The global fold of the protein was calculated using the DIANA software package from a list of 968 distance constraints. The internal cavity volume, a feature common to all known ns-LTP structures, was estimated to be  $750 \text{ \AA}^3$  using the 'CAVITE' program. This model of the complex was obtained by inserting a lipid molecule in the cavity and was energy minimized. The study showed that the protein fold described for the free form was only weakly affected by the insertion of the bulky lipid. Observation of some intermolecular NOEs between the protein and the lipid glycerol moiety revealed that the cavity entrance was located between residues His<sup>35</sup> and Arg<sup>44</sup>. The resulting solution structure was compared to the crystal structure of the maize ns-LTP/palmitate complex.

© 1997 Federation of European Biochemical Societies.

**Key words:** Wheat; Non-specific lipid transfer protein; Plant; Dimyristoylphosphatidylglycerol; Nuclear magnetic resonance; Fluorescence

## 1. Introduction

Lipid transfer proteins (LTPs) are ubiquitous proteins found in numerous living organisms which facilitate lipid exchange between natural and/or artificial membranes *in vitro*. Plant LTPs exhibit broad affinity for various lipids so that they are currently named non-specific LTPs (ns-LTPs). They form a family of proteins characterized by a molecular weight around 9 kDa, a basic pI and a highly conserved three-dimensional structure stabilized by four disulfide bonds. The biological function of plant ns-LTPs remains to be elucidated. Initially, they were thought to participate in the intracellular traffic of lipids. Such a role seems unlikely since it is recognized that these proteins are exported and are mainly located in the cell wall. Therefore, other roles, such as a participation in the formation of cutin layers or in the plant defence against phytopathogens, have been suggested (see [1] for a recent review). We have established the first three-dimensional structure of a ns-LTP isolated from wheat seeds by  $^1\text{H}$  multidimensional NMR [2]. This has revealed a new fold involving four

helices and a C-terminal fragment organized around a long internal cavity which has been suggested to be the lipid binding site. This type of organization was then confirmed with the maize ns-LTP structure that we established in solution [3] and in crystal by Shin et al. [4] and more recently with the barley ns-LTP structure [5]. The crystal structure of the complex of the maize protein with palmitic acid [4], the solution structure of its complex with 1-palmitoyl-2-lysophosphatidylcholine [3] and the barley ns-LTP complex with palmitoyl-CoA [6] demonstrated the capacity of ns-LTPs to incorporate a long fatty acid chain in their internal cavity. In the present work and in contrast with previous conclusions provided by the study of barley ns-LTP [6], we demonstrate that the wheat ns-LTP can also incorporate 1,2-dimyristoylphosphatidylglycerol (DMPG) which bears two acyl chains as natural lipid components recovered in cell membranes.

## 2. Materials and methods

### 2.1. Purification of wheat ns-LTP

Wheat ns-LTP was extracted from wheat seeds (*Triticum aestivum* L., cv. Etoile de Choisy) and purified according to a procedure previously described [7]. Its purity was above 95% as estimated from reversed-phase HPLC on a  $5\mu$  100A bonded silica column ( $25 \times 0.75$  cm) using a gradient of water-acetonitrile-0.05% TFA (1% acetonitrile/min) performed at 55°C.

### 2.2. Lipid binding by fluorescence spectroscopy

DMPG multilamellar vesicles (MLV) were prepared by vortexing DMPG (10 mg/ml) above its transition temperature (23°C) in 50 mM sodium phosphate buffer pH 7.0 and freeze thawing. To obtain homogeneously sized small unilamellar vesicles (SUV), DMPG multilamellar vesicles were sonicated at 4°C for 30 min using a Branson sonicator. Titanium particles were removed by filtration on a  $0.2 \mu\text{m}$  Millipore filter. Lipid titration of wheat ns-LTP was carried out by fluorescence spectroscopy as previously described [3]. The dissociation constant ( $K_d$ ) and the number of binding sites ( $n$ ) were determined by fitting experimental curves with a non-cooperative model assuming independent and identical sites [8].

### 2.3. NMR spectroscopy and molecular modelling

All NMR experiments were carried out on a 3 mM protein sample at 308 K and at a pH of 6.0. The complexation of the protein was obtained by  $\mu\text{l}$  addition of a solution of DMPG liposomes in the NMR tube containing the protein solution by steps of 0.2 equivalent. For each addition, one 1D and one TOCSY spectra were recorded. Complexation was achieved when a ratio of 1.2 DMPG molecule per protein molecule was reached. Then, the tube was argon filled and sealed. For assignment purposes, a P-COSY [9], a 90 ms mixing time clean TOCSY [10] and a 200 ms mixing time NOESY [11] spectra were recorded on a 500 MHz Bruker spectrometer equipped with a 3 axis field gradient unit. For each experiment, the water signal was suppressed just before the FID acquisition using the WATERGATE pulse sequence [12] where the selective 180° pulse was replaced by the 3-9-19 pulse sequence [13]. For the TOCSY and P-COSY spectra, a

\*Corresponding author. Fax: (33) 2 38 63 15 17.  
E-mail: sodano@cncrs-orleans.fr

supplementary weak power presaturation (approximately 10 Hz) during the relaxation period followed by a SCUBA sequence was used to further reduce the water signal. A NOESY spectrum with a mixing time of 60 ms was recorded for the NOE peak integration. Zero quantum contributions which are important in such a short NOESY mixing time were suppressed by a 10 ms magic angle spin-lock just before the FID acquisition [14]. All spectra were recorded with  $2048 \times 650$  data points and were zero-filled before Fourier transform to give  $2048 \times 1024$  real data point spectra except the 60 ms mixing time NOESY spectrum which was recorded with  $4096 \times 650$  data points and zero-filled to give a  $4096 \times 1024$  real data point spectrum. The  $^1\text{H}/^2\text{H}$  exchange experiment was performed as follows: a freshly lyophilized sample of the complexed protein was dissolved in  $\text{D}_2\text{O}$  at 273 K. After pH correction to a value of 6.0, the sample was placed in a preshimmed spectrometer at 308 K. Ten minutes after protein dissolution, a series of 1D experiments was recorded during 10 min. Then a 4 h NOESY experiment was acquired followed by an overnight NOESY experiment. Amide protons present in this latter experiment were considered as slowly exchanging. A 1D version of the heteroTOCSY experiment [15] was run on the  $\text{D}_2\text{O}$  protein sample to deduce proton resonances of the two glycerol moieties via the TOCSY transfer from the phosphorus nucleus. The mixing time of 40 ms was achieved with a MLEV16 pulse sequence [16].

The protein proton assignments were conducted using the EASY program [17]. The integrated volumes were converted into distances using the CALIBA program [18] with the strongest  $\text{NH}_{(i)}/\text{NH}_{(i+1)}$  connectivity in regular helices as distance reference. An upper limit of 5.0 Å was considered for the weakest volumes. A 200 ms mixing time NOESY spectrum was also used for the modelling study. Only cross-peaks present in this spectrum and absent in the 60 ms mixing time NOESY were considered. A fixed distance of 6.0 Å was associated with these new cross-peaks regardless of their volume intensity in order to take account of spin diffusion effects. Moreover,  $61 \text{ } ^3\text{J}_{\text{C}\alpha\text{H}\text{NH}}$  coupling constants were obtained from in-phase NOESY cross-peaks using the INFIT program [19]. These data together with the NOEs were used to generate angle constraints on  $\phi$ ,  $\psi$  and  $\chi^1$  angles using the HABAS program [18]. The distance constraint list generated by CALIBA and filtered by DIANA [18] resulted in a set of 968 constraints. The structure of the complexed protein was calculated from 200 random structures generated by DIANA. The 30 best structures with the lowest target function were used for further assignments of the ambiguous NOESY cross-peaks using the ASNO program [20]. At the end of the process, the 10 best DIANA structures whose target function ranged from 4.8 to 5.7 Å<sup>2</sup> were considered to be representative of the solution structure of the complex.

The best DIANA structure was used to build a preliminary structure of the complex with DMPG via the SYBYL software (Tripos, St. Louis, MO, USA) on a SILICON GRAPHICS workstation as follows: the use of the program 'CAVITE', which delineates cavity inside protein structures [21], defined a large hydrophobic cavity in the interior of the DIANA structure where both chains of the lipid were inserted. The orientation of the lipid was deduced from intermolecular NOEs between the lipid glycerol moieties and side-chain protons of residues His<sup>35</sup> and Arg<sup>44</sup>. Thereafter, the resulting structure was subjected to energy minimization using the TRIPOS force field, Kollman charges and a distance dependent dielectric constant,  $\epsilon = 4^*r$  in order to mimic the charge screening in an aqueous environment. During this minimization, the 968 distance constraints obtained from DIANA were applied.

### 3. Results

The binding study by fluorescence spectroscopy was performed with both multilamellar and small unilamellar vesicles. In both cases, the interaction of DMPG with wheat ns-LTP induced a 200% increase of tyrosine fluorescence intensity which allowed the determination of bound protein fraction  $\alpha = (F - F_0) / (F_{\text{max}} - F_0)$  (Fig. 1). By fitting the experimental data  $\alpha$  and  $R_i$ , the lipid to protein molar ratio, with the equation characterizing a non-cooperative model with independent and identical sites previously described [8], it was possible to determine the number of binding sites  $n$  and the dissociation

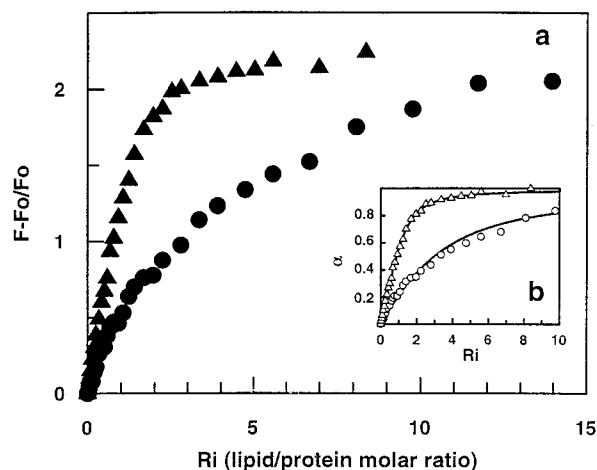


Fig. 1. Fluorescence titration curves of wheat ns-LTP with DMPG organised in SUV ( $\blacktriangle$ ) and MLV ( $\bullet$ ). a: Experimental data of the relative increase of fluorescence intensity. b: Fitted curves considering the fraction of bound protein  $\alpha$ .

constant,  $K_d$ . For SUV, a  $K_d$  of  $7.5 \pm 0.5 \mu\text{M}$  and a number of binding sites  $n$  of  $1.3 \pm 0.04$  were returned while for MLV the fitting produced  $K_d$  and  $n$  values of  $35.7 \pm 10.8 \mu\text{M}$  and  $2.5 \pm 0.4$ , respectively. Finally, the fitting was better with SUV than with MLV as assessed by  $\chi^2$  analysis.

The NMR study of complexation of DMPG by wheat ns-LTP was performed as follows. Evolutions of chemical shifts, line widths, scalar and dipolar connectivities were followed on TOCSY and NOESY  $^1\text{H}$  spectra during the titration of wheat ns-LTP by DMPG. Addition of the lipid,  $R_i$  ranging from 0.0 to 1.4, induced the splitting of many resonances into two components. One of these components increased with  $R_i$  and reached a plateau for  $R_i$  greater than 1.2 while the second one evolved in the opposite direction. An example is given in Fig. 2 where the TOCSY connectivities between NH and  $\beta$  protons of Tyr<sup>79</sup> are plotted for a ratio  $R_i = 0.5$  for which the two forms of the protein are present in solution at equal amounts. These results were the first clue to the formation of a 1/1 complex and a slow exchange rate on the NMR time scale between the free and complexed forms of the protein. It is noteworthy that both  $\beta$  protons of Tyr<sup>79</sup> which had degenerate resonances in the free form were well separated in the complexed form (Fig. 2).

The protein proton chemical shifts were deduced primarily from a thorough analysis of the TOCSY and NOESY spectra and the cross-peak line-shapes. Proton frequency and cross-peak line-shape were used so as to discriminate between protein and lipid resonances. Unfortunately, it appeared that most of the protons of the lipid chains had degenerated frequencies. Therefore, the observed intermolecular NOEs between both myristoyl chains and the protein were not considered during the course of the protein modelling. The sequential assignment of the protein proton resonances was obtained according to standard procedures [22] and was primarily based on the  $^1\text{H}$  NOESY spectrum. Four helices were readily detected through the observation of strong  $\text{NH}_{(i)}/\text{NH}_{(i+1)}$  and  $\text{C}\alpha\text{H}_{(i)}/\text{NH}_{(i+3)}$  connectivities. In the global fold issued from modelling, they encompassed residues from His<sup>5</sup> to Val<sup>17</sup> for H1, from Gln<sup>26</sup> to Asp<sup>36</sup> for H2, from Gln<sup>41</sup> to Ala<sup>55</sup> for H3 and from Glu<sup>63</sup> to Cys<sup>73</sup> for H4. The first three helices were almost parallel, describing an up-down-up

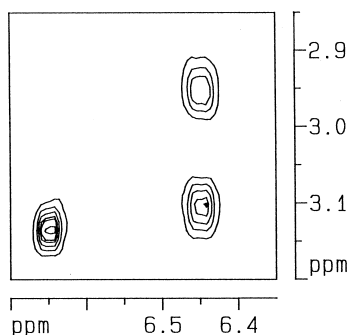


Fig. 2. Region of a TOCSY spectrum displaying the relayed scalar connectivities between the amide and the  $\beta$  protons of Tyr<sup>79</sup> for a  $R_i$  value of 0.5. At this lipid concentration, both protein forms, free and complexed, are present in solution at nearly equal amounts.

motif, while the fourth helix was globally perpendicular to the first three. The C-terminal region was devoid of any regular hydrogen bonded canonical structure except for a  $\beta$ -turn involving residues 82–85 and ran parallel to H4 from residues 77 to 83 and then to H3 from residue 84 to the C-terminal residue. The protein scaffold which was common to all available ns-LTP structures [3–5] was maintained by a network of four disulfide bridges distributed in pairs on two protein poles, providing great stability to this protein. The RMSD calculated on the heavy atoms of the backbone of the four helices relative to the mean structure is 0.75 Å which is indicative of a moderate resolution solution structure. The 10 best structures, shown in Fig. 3A, satisfied the NMR constraints since the average number of violations higher than 0.3 Å was 1.1 per structure. The main contributions to the target function values arose from van der Waals contacts

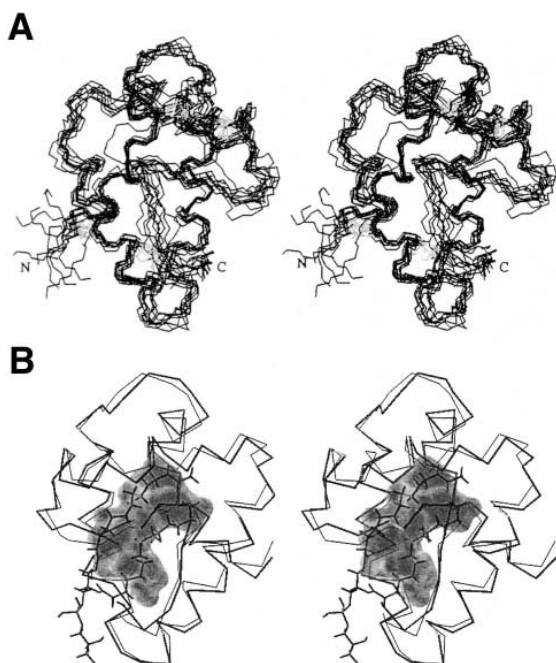


Fig. 3. A: Superposition of the 10 best DIANA structures fitted on the backbone heavy atoms of the first three helices. B: C $\alpha$  trace of the complexed structure (thin lines) with the DMPG molecule (bold lines). The trace of the hydrophobic pocket calculated on the DIANA structure before the insertion of the lipid is also shown.

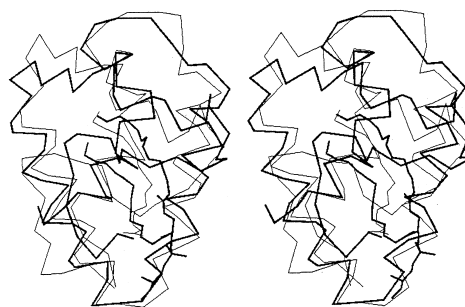


Fig. 4. Superposition of the solution structure of wheat ns-LTP complexed with DMPG (bold lines) and the X-ray structure of maize ns-LTP complexed with a palmitate (thin lines).

between the prolines of the doublet Pro<sup>70</sup>-Pro<sup>71</sup> located at the end of the H4 helix.

The volume of the internal hydrophobic cavity occupied by the two myristoyl chains was estimated to be 750 Å<sup>3</sup> ( $\pm$  250 Å<sup>3</sup>) using the program 'CAVITE' [21]. The pocket was bordered by hydrophobic residues belonging to the four helices and to the C-terminal tail. Its mean direction was almost parallel to the bundle of the first three helices. The internal cavity was plugged on one side by the side-chains of residues Leu<sup>14</sup>, Val<sup>17</sup>, Ala<sup>55</sup>, Ile<sup>58</sup>, Leu<sup>61</sup> and Leu<sup>83</sup> and its entrance located between the C-end of H2, the N-end of H3 and Val<sup>90</sup>. As previously described in Section 2, a model of the complex was built, the hydrophobic cavity being large enough to accommodate both chains of the lipid. The resulting structure satisfied the NMR constraints since the observed number of distance violations higher than 0.3 Å was 6. The C $\alpha$  trace of the structure together with the lipid is shown in Fig. 3B.

#### 4. Discussion

The interaction of wheat ns-LTP with DMPG, a diacyl phospholipid forming liposomes, induces an increase of the intensity of protein tyrosine fluorescence as previously observed with lysoPC, a monoacyl phospholipid forming micelles. At lipid saturation, the relative increase of fluorescence intensity is identical whatever the lipid organization, SUV or MLV. This indicates that tyrosine residues are in the same lipid environment. However, lipid titration leads to different binding curves characterized by different  $K_d$  and  $n$ . It is important to keep in mind that two types of binding phenomena have to be considered with bilayer vesicles: (1) adsorption on the bilayer interface and (2) binding of a lipid molecule in the internal cavity. Both phenomena determine the binding constants,  $K_d$  and  $n$ . With monolayer techniques, it was previously shown that lipid packing determines the importance of each type of interaction [23]. In vesicles, lipid packing is related to bilayer curvature which is higher in SUV than in MLV. Furthermore, in contrast to SUV, MLV are composed of heterogeneously sized vesicles. In the case of SUV, the fitting of lipid titration curves provided a number of binding sites close to 1, suggesting that the binding constants are mainly driven by the binding of DMPG inside the cavity. In contrast,  $n$  was significantly above 1 for MLV, suggesting that interaction with bilayer interfaces and binding of DMPG in the internal cavity both determine the binding constants. In contrast to SUV, the tighter lipid packing in MLV creates an important energy barrier and for the largest MLV it is prob-

able that ns-LTP interacts only with the bilayer interfaces. Therefore, in contrast to SUV, it is necessary to add more MLV to saturate the binding cavity with DMPG: this leads to higher  $K_d$  and to a number of binding sites above 1. The NMR studies confirm the formation of a 1/1 protein complex in solution. This was evidenced by the protein titration by a DMPG solution and confirmed by the protein structure calculations: indeed, the calculated void volume present within the protein structure allows the entrance of only one DMPG molecule.

The three-dimensional structures of wheat, maize and barley ns-LTPs in the free form are very similar. In the two complexes of maize [3,4] and barley [6] ns-LTP with lipids, a single aliphatic chain was inserted in the internal cavity of these proteins which barely disturbs their three-dimensional structure. The present results provide the first evidence of the possibility of inserting a diacyl lipid inside the protein. Fig. 4 shows a superposition of the structures of wheat ns-LTP complexed with DMPG and the structure of the complex maize ns-LTP/palmitate. This comparison emphasizes that both protein structures bear very close resemblance at least on regular secondary elements. Indeed, the RMSD between these two structures calculated on the backbone heavy atoms of the four helices is 1.4 Å, indicating that the introduction of a bulky lipid like DMPG does not significantly deform the protein structure. The only noticeable difference concerns the C-terminal region. In fact, although the overall conformation of this segment is conserved in both structures, in the wheat ns-LTP complex, this segment from residue 77 to residue 83 is located closer to the H4 helix although pushed outwards into the solvent. This is evidenced by comparing Figs. 3A and 4. This different location seems to be associated with a steric hindrance between the side-chain of Tyr<sup>79</sup> and the glycerol group which bears the two lipidic chains on one hand and between the side-chains of Ile<sup>81</sup> and Leu<sup>83</sup> and the myristoyl chains on the other. This segment displacement is further supported by the disappearance of the NOEs between the Tyr<sup>79</sup> aromatic ring protons and the C-terminal residues of the H2 helix upon lipid complexation. Moreover, the insertion of the lipid in the interior of the protein induces some proton chemical shift variations which probe proton environment local changes. Interestingly, the most glaring amide proton frequency shifts are localized in the fourth helix and the C-terminal segment (data not shown).

In the present complex, the orientation of the lipid in the hydrophobic cavity stems from a few interprotein-ligand NOE contacts. Since most of the myristoyl protons share the same frequency, the relevant connectivities involve the side-chains of His<sup>35</sup> and Arg<sup>44</sup> and the glycerol moiety whose one proton resonates in a free spectral region. This lipid orientation is in agreement with that of palmitate in the complex of maize ns-LTP where a hydrogen bond between the hydroxyl of Tyr<sup>81</sup> and the lipid carboxylate was observed [4]. This hydrogen bond is not found in the DMPG complex structure even though one carbonyl of the two DMPG ester groups is similarly located. This absence results primarily from the displacement of the aromatic ring of Tyr<sup>79</sup> which is directed outwards into the solvent. Moreover, in both cases, the CH<sub>3</sub> lipid termini are situated very close to the side-chains of residues Leu<sup>14</sup> and Ile<sup>58</sup> between the C-ends of helices H1 and H3 on the opposite pole of the protein.

Concerning the lipid conformations, the aliphatic chains

adopt almost parallel orientations in both structures and follow the protein internal cavity shapes. The lipid chain conformations, albeit linear, are slightly curved in the X-ray and solution structures. Furthermore, the palmitoyl chain from carbon C1 to C9 is closely superimposed on the first nine carbons of the myristoyl chain which is the closest to the H3 helix. Then from C9 to C16 the palmitic chain location diverges and is located between the two aliphatic chains of DMPG.

Previous studies have shown that wheat ns-LTP was able to transfer DMPG between membranes [23]. A thorough analysis of the dimensions of the protein cavity showed that the volume is highly variable depending on small conformational changes of internal side-chains and backbone [21]. The present study shows that ns-LTPs are able to interact with both monoacyl and diacyl lipids and with both lipid forming micelles or lamellar liquid-crystalline phases. This is in agreement with the capacity of such proteins to enhance the transport of diacyl lipids between bilayer membranes. Furthermore, the NMR work demonstrates clearly that the complex between wheat ns-LTP and DMPG exists in solution and is stable enough to be studied and modelled. In addition, it shows that the insertion of such a bulky lipid does not produce significant structural deformations of the protein. The main observation is a displacement of the C-terminal region. This C-terminal segment, which was assumed to be involved in the interaction between the protein and the lipid layers [3], seems to play another important role in modulating the accessible cavity volume.

*Acknowledgements:* This work was supported by the Centre National de la Recherche Scientifique (C.N.R.S.), the Institut National de la Recherche Agronomique (I.N.R.A.), the Région Centre, the Région Pays de Loire and the Université d'Orléans.

## References

- [1] Kader, J.C. (1996) *Annu. Rev. Plant Physiol. Plant Mol. Biol.* 47, 627–654.
- [2] Gincel, E., Simorre, J.P., Caille, A., Marion, D., Ptak, M. and Vovelle, F. (1994) *Eur. J. Biochem.* 226, 413–422.
- [3] Gomar, J., Petit, M.C., Sodano, P., Sy, D., Marion, D., Kader, J.C., Vovelle, F. and Ptak, M. (1996) *Protein Sci.* 5, 565–577.
- [4] Shin, D.H., Lee, J.Y., Hwang, K.Y., Kim, K.K. and Suh, S.W. (1995) *Structure* 15, 189–199.
- [5] Heinemann, B., Andersen, K., Nielsen, P., Bech, L.M. and Poulsen, F.M. (1996) *Protein Sci.* 5, 13–23.
- [6] Lerche, M.H., Kragelund, B.B., Bech, L.M. and Poulsen, F.M. (1997) *Structure* 5, 291–306.
- [7] Desormeaux, A., Blochet, J.E., Pézolet, M. and Marion, D. (1992) *Biochim. Biophys. Acta* 1121, 137–152.
- [8] Dubreil, L., Compoin, J.P. and Marion, D. (1997) *J. Agric. Food Chem.* 45, 108–116.
- [9] Marion, D. and Bax, A. (1988) *J. Magnet. Reson.* 80, 528–533.
- [10] Gresinger, C., Otting, G., Wüthrich, K. and Ernst, R.R. (1988) *J. Am. Chem. Soc.* 110, 7870–7872.
- [11] Jeener, J., Meier, B.H., Bachmann, P. and Ernst, R.R. (1979) *J. Chem. Phys.* 71, 4546–4553.
- [12] Piotto, M., Saudek, V. and Sklenar, V. (1992) *J. Biomol. NMR* 2, 661–665.
- [13] Sklenar, V., Piotto, M., Lepik, R. and Saudek, V. (1993) *J. Magnet. Reson. Ser. A* 102, 241–245.
- [14] Mitschang, L., Keeler, J., Davis, A.L. and Oschkinat, H. (1992) *J. Biomol. NMR* 2, 545–556.
- [15] Kellogg, G.W. (1992) *J. Magnet. Reson.* 98, 176–182.
- [16] Levitt, M.H., Freeman, R. and Frenkiel, T. (1982) *J. Magnet. Reson.* 47, 328–330.

- [17] Bartels, C., Xia, T.-E., Billeter, M., Güntert, P. and Wüthrich, K. (1995) *J. Biomol. NMR* 5, 1–10.
- [18] Güntert, P., Braun, W. and Wüthrich, K. (1991) *J. Mol. Biol.* 217, 517–530.
- [19] Szyperski, T., Güntert, P., Otting, G. and Wüthrich, K. (1992) *J. Magnet. Reson.* 99, 552–560.
- [20] Güntert, P., Berndt, K. and Wüthrich, K. (1993) *J. Biomol. NMR* 3, 601–606.
- [21] Gomar, J., Sodano, P., Sy, D., Shin, D.H., Lee, J.Y., Suh, S.W., Marion, D., Vovelle, F. and Ptak, M. (1997) to be published.
- [22] Wüthrich, K. (1986) *NMR of Proteins and Nucleic Acids*, Wiley Interscience, New York.
- [23] Subirade, M., Salesse, C., Marion, D. and Pérolet, M. (1995) *Biophys. J.* 69, 974–988.